

# PERFORMANCE ENHANCEMENT OF THE SENSORLESS DRIVE FOR BRUSHLESS DC MOTORS USING KALMAN FILTER

Hyeong-Gee Yeo, Tae-Hyeong Kim, Jung-Bae Park, Kwang-Woon Lee, Ji-Yoon Yoo  
School of Electrical Engineering, Korea University

5-1, Anam-Dong, SungBuk-Gu, Seoul, 136-701, Korea, Phone:+82-2-921-5588 FAX:+82-2-921-0163

**ABSTRACT** - Indirect sensing of the rotor position of permanent magnet brushless DC motors contains position error. Such measuring error can be attenuated by adopting Kalman filter. In this paper, the cause of measuring error is analyzed and the design technique of Kalman filter is described. Experimental results show that the proposed sensorless drive exerts superior performances.

## I. INTRODUCTION

Permanent magnet brushless DC motors have found wide application due to their high power density and ease of control. Moreover the machines have high efficiency over wide speed range. Therefore, it is suitable for variable speed applications and results in energy saving[1].

Generally the drive for the brushless DC motor requires a position sensor for providing proper commutation sequence to turn on the power devices in the inverter bridge. But the sensor increases cost and size of the motor. In addition, it reduces the system ruggedness and complicate the motor configuration. Especially, the application such as completely sealed compressor cannot adopt the position sensor because of its low reliability. Due to these limitations of the motor operation with position sensor, the sensorless drive technique of brushless DC motors is receiving wide attention.

Up to now, various methods for indirect sensing of the rotor position are developed. Typical indirect sensing algorithms reported in literatures are terminal voltage sensing[2], terminal current sensing[3], third harmonic voltage integration[4] and back emf integration[5].

These methods can be classified into two groups by

implementations. One group directly detects the commutation time through integration of back-EMF. But the other group detects the time when the back-EMF of the open phase becomes zero, and then calculates the commutation time.

In brushless DC motors, in normal operation range, the commutation positions always lag  $30^\circ$  in electrical angle than zero-crossing positions. But field weakening mode or interior permanent magnet(IPM) type machine, it is recommended that the commutation angles lag less than  $30^\circ$  than zero-crossing angles[6,7].

The integration method cannot provide adjustable commutation scheme because it directly detects the commutation angle which always lags  $30^\circ$  than zero-crossing position. Therefore, the zero-crossing detection method is more preferred than the integration method. However, the detection of zero-crossing is restricted during PWM duty cycle. This limitation of detection deteriorates the sensing resolution of rotor position. Thus the sensing resolution depends on PWM duty cycle and on the number of PWM pulses per revolution. Especially, at high speed, the number of PWM pulses per one revolution decreases severely, and the resolution decreases.

In this paper, a method utilizing Kalman filter is proposed for compensation of low resolution. For applying the method, an indirect position sensing method using terminal voltage is presented and a simple sensorless drive is implemented. And then the proposed filtering method is applied to the sensorless drive. Experimental results are shown to confirm the feasibility of the method and the validity of the sensorless drive. It will be shown that the proposed system extends the operation range and have robustness over step change of load torque.

## II. INDIRECT POSITION SENSING METHOD

Figure 1 shows a equivalent circuit of brushless DC motor and inverter system. In general, only two of the three phases are excited at any instant and a phase remains open as shown in figure 2. The phase EMF reverses its polarity during open and crosses the point where EMF is zero. The rotor position at which EMF becomes zero is zero-crossing point(ZCP). The amplitude of EMF is proportional to rotor speed, but ZCPs are invariant. For proper commutation, the open phase should be excited at 30° phase delay after ZCP.

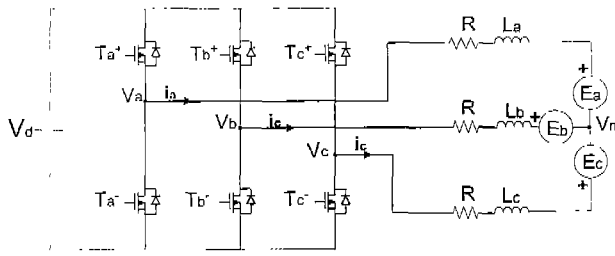
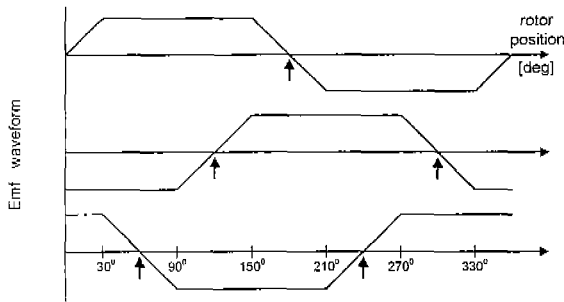


Fig.1 Equivalent circuit of brushless DC motor and inverter



active phase	c+	a+	b+	c+	a+	b+
open phase	a	c	b	a	c	b

Fig2. Emf and inverter state (arrows indicate zero crossing points of Emf waveforms)

Terminal voltage waveform of the open phases are closely related to the PWM strategy. In this paper, as shown in figure 3, limited unipolar PWM strategy is selected for minimizing the current ripple and switching loss of switching devices[5].

Let's examine the terminal voltage of open phase when the rotor position is between 210° and 270° (see fig.2

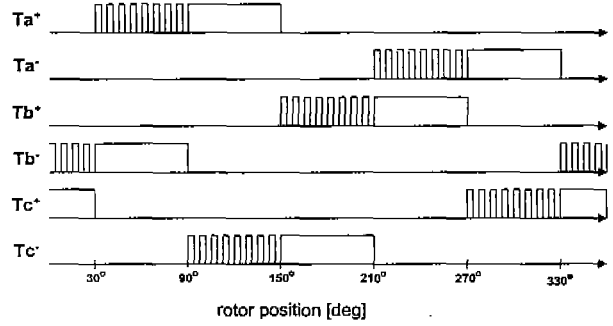


Fig 3. Switching patterns of inverter

and fig.3). At that region, phase A and B are excited and phase C remains open. The switch device  $T_a^-$  turns on and off according to PWM,  $T_b^+$  remains on, and all the others remain off. When  $T_a^-$  turns on, the circuit equation of figure 1 is

$$V_d = Ri + L \frac{di}{dt} + e_a - e_b + L \frac{di}{dt} + Ri \quad (1)$$

where  $V_d$  is DC link voltage,  $R$  is phase resistance,  $L$  is phase inductance,  $i$  is line current and  $e$  is phase EMF. At the region,  $e_a$  equals to  $-e_b$ . Therefore, the potential of neutral,  $v_n$  is

$$v_n = \frac{1}{2} V_d. \quad (2)$$

Since the terminal voltage of the open phase C is the sum of  $v_n$  and EMF of phase C, we have

$$v_c = \frac{1}{2} V_d + e_c. \quad (3)$$

When  $T_a^-$  turns off, the exciting current circulates through  $T_b^+$  and  $D_a^+$ . Now, the circuit equation is written as

$$0 = Ri + L \frac{di}{dt} + e_a - e_b + L \frac{di}{dt} + Ri \quad (4)$$

And the terminal voltage is written as

$$v_c = e_c. \quad (5)$$

The ZCPs can be detected where the terminal voltage  $v_c$  equals to zero or  $v_d/2$  according to the PWM signal. It is strongly recommended to detect the terminal voltage only when PWM signal is high because sensing circuit

may be saturated when terminal voltage is low. Fig.4 shows the sensing technique using the terminal voltage waveform.

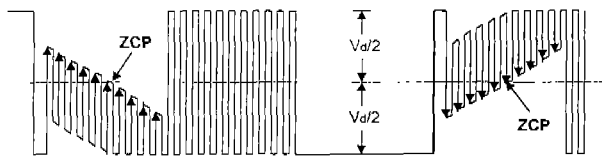


Fig 4. Waveform of terminal voltage

### III. COMPENSATION OF POSITION ERROR

After detection of ZCP, the commutation time  $t_c(k)$  can be calculated as

$$t_c(k) = t_{ZCP}(k) + \frac{1}{2} \Delta t_{ZCP}(k) \quad (6)$$

$$\Delta t_{ZCP} = t_{ZCP}(k) - t_{ZCP}(k-1) \quad (7)$$

where  $t_{ZCP}(k)$  is the time when a ZCP is detected. But, as described in the previous section, the detection of  $t_{ZCP}(k)$  contains measuring error because it can be detected only during PWM duty cycle. At high speed, the number of PWM pulses decreases during one revolution. Thus the measuring error increases according to rotor speed. For example, at 4,500 rpm, 5 kHz PWM carrier, and 3 phase 4 pole motor, one carrier pulse induces position error at maximum  $20^\circ$  in electrical angle.

The measuring error of ZCP can be attenuated by applying the scalar Kalman filter to first order Weiner process model.

$$\begin{aligned} P_{k+1}^- &= \Phi_k P_k \Phi_k^T + \Phi_k \\ \hat{x}_{k+1} &= \Phi_k \hat{x}_k \\ K_{k+1} &= P_k^- H_k^- (H_k^- P_k^- H_k^- + R_k)^{-1} \end{aligned} \quad (8)$$

$$P_k = (1 - K_k H_k) P_k^-$$

$$\hat{x}_k = \hat{x}_{k-} + K_k (Z_k - H_k \hat{x}_{k-})$$

where  $P_k$  means error covariance and  $K_k$  means Kalman gain.  $Q_k$  and  $R_k$  mean covariance of system

noise and measurement noise, respectively.

The larger  $Q_k$ , the heavier the weight of process model becomes. On the other hand, the larger  $R_k$ , the heavier the weight of measured value  $t_{ZCP}(k)$ . The measurement noise of  $t_{ZCP}(k)$  becomes large as speed goes up. Therefore, the weight of process model  $R_k$  must have relatively large value at high speed region. On the contrary,  $Q_k$  must have relatively large value at low speed region.

Figure 5 shows a simulation result of Kalman filtering. At low speed, The filtered value  $\Delta \hat{t}_{ZCP}(k)$  approximates to measured value  $\Delta t_{ZCP}(k)$ . At high speed,  $\Delta \hat{t}_{ZCP}(k)$  approximates to average value of  $\Delta t_{ZCP}(k)$  s.

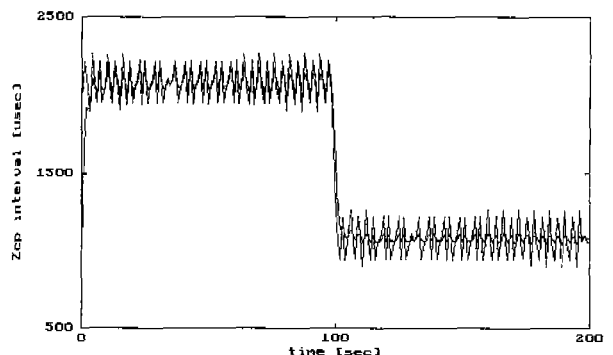


Fig 5. Filtering result

### IV. EXPERIMENTAL RESULT

A sensorless drive is implemented as shown in figure 6. The outputs of three ZCP detection circuits detect zero-crossing of each phase by transition at ZCPs, and acquaint to microprocessor. Then, the microprocessor calculates  $t_{ZCP}(k)$ ,  $\Delta t_{ZCP}(k)$  and  $\Delta \hat{t}_{ZCP}(k)$ . Finally, the commutation time  $t_c(k)$  is calculated as

$$t_c(k) = t_{ZCP}(k) + \frac{1}{2} \Delta \hat{t}_{ZCP}(k) \quad (9)$$

The specs and parameters of BLDC motor are represented in table 1.

Figure 7 show terminal voltage and phase current waveforms without and with Kalman filter. In case of without filtering, it can be observed that the conduction angles mismatch with phase EMFs. The mismatch

becomes large as speed goes up. Since severe mismatch between phase EMF and conduction angle induces over current fault, it is impossible to operate over 3,600 rpm. In case of applying Kalman filter, the conduction angles matched relatively well with phase EMF. Speed operation range is extended up to 4,500 rpm. Figure 8 shows the waveforms when operating at 4,500 rpm. Using 16 MHz 87c196mc microprocessor, it needed only 120  $\mu$ s for the calculation of scalar Kalman filter.

One of the major reason that adoption of Kalman filter is its superior characteristics of transient response. Static filters such as Butterworth or Chevycheff have poor transient response. When step change of load or speed command, phase margin characteristic of static filters may induce the loose of synchronism. Figure 9 shows speed and phase current response of proposed drive system when step increase of load torque(0.54 Nm) for 5 seconds. The synchronism is maintained well in spite of step load.

Table 1. Specs and parameters of BLDC motor

Phase / pole	3/4
Input voltage	AC 110 V
Rated current	3.44 A
Rated output	300W
Rated/maximum speed	3,000/4,500 rpm
Rated torque	0.95 Nm
Torque constant	0.29 Nm/A
Inertia	0.000083 Kgm <sup>2</sup>

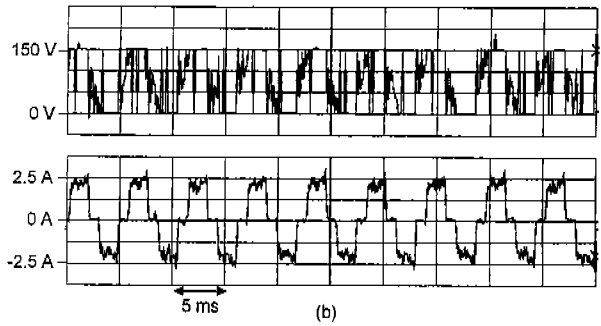
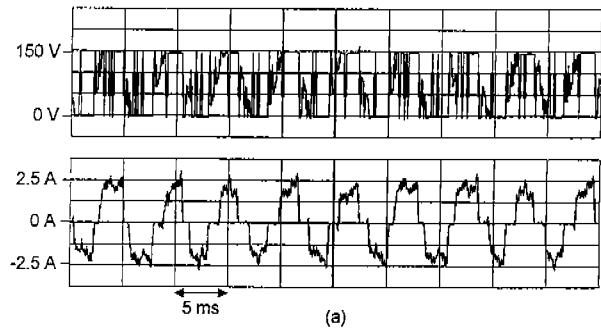


Fig.7 Waveforms of Terminal voltage and phase current at 3,600 [rpm], (a) without filter, (b) with Kalman filter

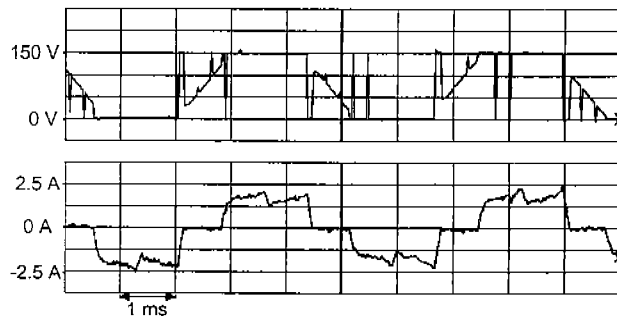


Fig.8 Terminal voltage and phase current waveform at 4,500 [rpm]

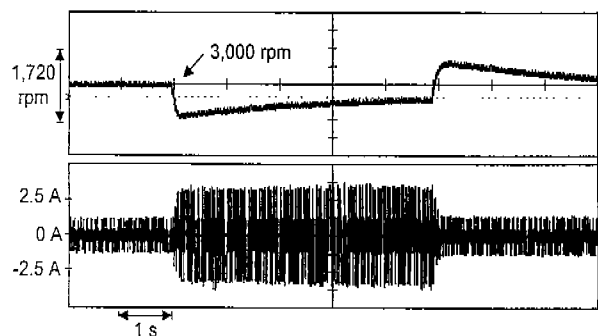


Fig.9 Speed and phase current response for step load

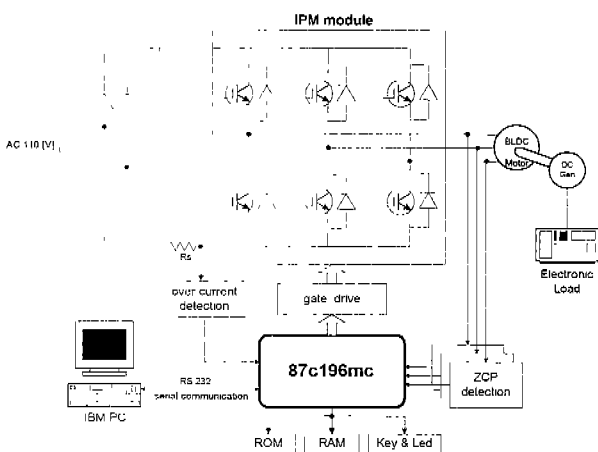


Fig 6. Motor-drive system configuration

## V. CONCLUSION

In this paper, the source of measuring error of sensorless BLDC motor drive which detects zero-crossing position is analysed. An effective method which can attenuate the measuring error is proposed using Kalman filter. Using a 16-bit microprocessor, a simple and economical sensorless drive is implemented and experimented. Without filtering, sensorless operation range is limited about 3,600 rpm. But with Kalman filter, operation range is extended up to 4,500 rpm. Moreover, the proposed system maintained synchronism safely even on the step change of load torque.

## REFERENCES

- [1] Electrical Power research, *Electric Motors; Markets, Trends, and Applications, 1992*
- [2] K.Iizaka, H.Uzuhashi, et.al., "Microcomputer Control for Sensorless Brushless DC Motor," IEEE Trans. on Industry Applications, vol. IA-21, No. 4, pp.595-601, May/June 1985
- [3] S.Ogasawara and H.Akagi, "An Approach to Position Sensorless Drive for Brushless DC Motor," Conference Record of the 1990 IEEE Industry Applications Society Twenty fifth IAA Annual Meeting, pp. 443-447, 1990
- [4] J.C.Moreira, "Indirect Sensing for Rotor Flux Position of Permanent Magnet AC Motors Operating in a Wide Speed Range," Conference Record of the 1994 IEEE Industry Applications Society Twenty forth IAA Annual Meeting, pp. 401-407, 1994
- [5] R.C.Becerra, T.M.Jahns and M.Ehsani, "Four-Quadrant Sensorless Brushless ECM Drive," 6th Annual Applied Power Electronics Conference and Exposition, pp.202-209, 1991
- [6] R. F. Schiferl and T. A. Lipo, "Power Capability of Salient Pole Permanent Magnet Synchronous Motors in Variable Speed Drive Applications", IEEE Trans. on Ind. Appl., vol. 26, no. 1, pp. 681-689, Jan./Feb. 1990.
- [7] S. Morimoto, et. al., "Optimum Machine Parameters and Design of Inverter-Driven Synchronous Motors for Wide Constant Power Operation", Conf. Rec. of IEEE IAS, pp. 177-182, 1994.